Integrated Optical Setups for Characterizing and Stabilizing Polarization States of Light

Abstract: The ability to characterize and stabilize light polarization states initiates the development of optical technologies which will yield tremendous societal impacts. Multiple platforms aimed to control the state of polarization have been proposed but lack stability and tunability for experimental implications. This study developed optical setups that are easily constructed and operated to precisely measure and stabilize polarization states. Photon pulses were produced using independent Acousto-Optic Modulator and Electro-Optic Modulators units, where an applied voltage (0-500V) encoded a desired polarization state. Photon characterization incorporated a Quarter-Wave Plate (QWP), Linear Polarizer, and Detector. Stokes Parameters of light were evaluated via a Fourier transformation and best-fit curve of the transmitted light intensity/integrated photon counts concerning the QWP angle. To stabilize drifted polarization, a 4x4 Mueller matrix determined the required angles for a QWP and half-wave plate (HWP) setup. The experimental S_1 parameter outputs for H and V were 0.9592 ± .0044 and -1.0047 ± .0002, respectively. The experimental S_2 parameter outputs for D and A were 0.99245 ± 0.00535 and -0.98645 ± 0.01215, respectively. The experimental S_3 parameter outputs for R and L were 0.81395 ± .00685 and -0.7415 ± 0.0108, respectively. Experimental verifications rendered precision and accuracy of the input polarization. After calculating the drifted polarization, the QWP and HWP setup stabilized polarization. This study developed a polarization detection and stabilization system that could be applied in fabricating optical technologies. Future works include incorporating optical detection signals to characterize and stabilize light polarization simultaneously.

1. INTRODUCTION:

The polarization states of light reveal essential findings for many scientific and technological applications [1-5]. Light polarization provides details on the size and distribution of particles in the atmosphere [2], isolates synthetic materials from natural surfaces [3], exhibits intelligence about the interactions between excited states of atoms [4], and issues disease diagnostics by measuring scattered light in biological tissue [5]. Polarized light also encodes and transmits information for optical communications [6]. Detecting and stabilizing light polarization is currently limited by the inability to measure high frequency and low intensity pulses and to retain polarization upon transmission in optical fibers [6,7], impeding the development of essential optic-based technologies.

Polarization State Production and Measurement

Optical modulators are widely used to produce polarization states due to the tuning ability of experimental variables, including light frequency and intensity. However, the stability of optical modulators is susceptible to arbitrary factors such as temperature changes which hinder polarization generation [8,10]. Aillerie *et al.* [8] demonstrated the thermo effects in electro-optic systems, signifying that upon miniscule temperature changes, dramatic variations in birefringent material are associated with the same applied voltage to create a distinct polarization. The inability to sufficiently generate a polarization has implications in measurements. Moreover, individualizing each polarization parameter is essential in characterizing the state. Commercial polarimeters only confirm whether or not a polarization is present instead of quantitatively assessing the amount of a particular polarization [9-12]. Conventional methods such as dividing amplitude based on four-detectors demonstrate adjustment difficulties, have delayed response times, and are unable to be tuned for varying experimental necessities [13-18].

Polarization Transmission Along Optical Fibers

Optical fibers are useful in long and short propagation distances. However, small birefringent effects within the fiber and external perturbations describing the physical environment cause polarization to drift [19-21]. Multiple fibers have been reconstructed over the past decades to maintain polarization but are limited by supporting only a single polarization [22-24]. Optical communications involve sequences of altering polarizations, thereby utilize single-mode non-polarization-maintaining optical fibers, despite an essential component of retaining their polarized state [25-30]. Thus, a stringent condition is to stabilize the drift in polarization when light is transmitted through optical fibers.

This study had two primary goals: to develop an executable code for characterizing light polarization states using Stokes parameters via (i) a fitted curve and (ii) a Fourier transformation technique and secondly, to incorporate a waveplate setup in which the required angles to compensate for changes in polarization are determined using Stokes/Mueller calculus.

2. METHODOLOGY:

2.1 *Stokes Parameters/Poincaré Sphere*

Light of any particular polarization (fully polarized, partially polarized, or unpolarized) is able to be characterized by four individual parameters, using the equations:

$$S_0 = S_0\,(0°) + S_0\,(90°) = S_0\,(45°) + S_0\,(-45°) = S_0\,(\mathrm{RHC}) + S_0\,(\mathrm{LHC})$$

$$S_1 = S_0\,(0°) - S_0\,(90°)$$

$$S_2 = S_0\,(45°) - S_0\,(-45°)$$

$$S_3 = S_0\,(\mathrm{RHC}) - S_0\,(\mathrm{LHC})$$

S_0 represents the intensity of the light, which is requisite in determining other polarization parameters; S_1 describes the preponderance of horizontally (H) polarized light over vertically (V) polarized light; S_2 describes the preponderance of diagonally (D) polarized light over anti-diagonally (A) polarized light; and S_3 describes the preponderance of right handed circularly (RHC) polarized light over left handed circularly (LHC) polarized light. The Poincaré sphere (Figure 1) was used to describe possible polarizations where the length of a vector reaching a point on or within the sphere represents a full or partial polarization, respectively. The alteration in polarization may be represented by the change in length and/or direction of a vector within the sphere.

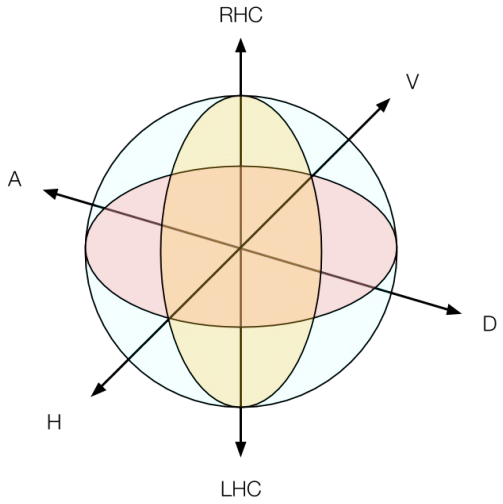

Figure 1: Poincaré sphere describes polarization parameters. Image developed by student author.

2.2 *Stabilization of Light Polarization*

Polarization Drift

The polarization generation source was used to encode desired polarizations. Upon characterization, the polarized pulses were delivered to Figueroa's graduate laboratory using a $30m$ long single-mode non-polarization-maintaining optical fiber from Figueroa's undergraduate laboratory (Thorlabs, S630-HP) to determine changes in polarization. After retrieval, the polarization drift was calculated by averaging the BFC and FT polarization parameter which described the inputted polarization and then subtracting the averaged polarization parameters before and after passing the optical fiber.

Stabilization Setup

A setup comprising a QWP followed by a half-wave plate (HWP) compensated for the change in polarization. To determine the required angles of the wave plates necessary for stabilizing the drift:

$$\vec{S}_{out} = M_2 * M_1 * \vec{S}_{in}$$

where S_{out} describes the ideal (theoretical) polarization to output, M_2 describes the Mueller matrix of the HWP, M_1 describes the Mueller matrix of the QWP, and S_{in} describes the inputted (experimentally drifted) polarization to stabilize.

The Mueller matrix of a HWP is given by:

$$M_2 = \begin{pmatrix} 1 & 0 & 0 & 0 \\ 0 & \cos^2(2\theta_2) - \sin^2(2\theta_2) & 2\sin(2\theta_2)\cos(2\theta_2) & 0 \\ 0 & 2\sin(2\theta_2)\cos(2\theta_2) & \sin^2(2\theta_2) - \cos^2(2\theta_2) & 0 \\ 0 & 0 & 0 & -1 \end{pmatrix}$$

where θ_2 is the HWP angle. The Mueller matrix of a QWP is given by:

$$M_1 = \begin{pmatrix} 1 & 0 & 0 & 0 \\ 0 & \cos^2(2\theta_1) & \sin(2\theta_1)\cos(2\theta_1) & -\sin(2\theta_1) \\ 0 & \sin(2\theta_1)\cos(2\theta_1) & \sin^2(2\theta_1) & \cos(2\theta_1) \\ 0 & \sin(2\theta_1) & -\cos(2\theta_1) & 0 \end{pmatrix}$$

where θ_1 is the QWP angle.

To calculate θ_1 and θ_2 for stabilizing polarization, S_{in} is written as a 4x1 matrix and multiplied with the equation in order to obtain the theoretical S_{out} value. All experimental S_{out} (ideal polarization) values were compared to the experimental S_{in} (drifted polarization) values using the Poincaré sphere to describe the change in length of the polarization vector. H, V, D, and A polarizations were stabilized.

3. RESULTS/DISCUSSION:

Stabilizing Polarization

Polarization Drift of H, V, D, and A

An applied EOM voltage encoded a desired polarization. After characterizing the polarization using a QWP, linear polarizer, and standard photodetector, polarized pulses were delivered to another laboratory using a single-mode optical fiber. After retrieval, the polarization was characterized once again to measure for drift. H, V, D, and A states were characterized. The experimental drift measurements are shown in Table 1:

Table 1. Polarization Drift

Polarization	Drift caused by fiber
H	S_1 (Before fiber) $-$ S_1 (After fiber) $= 0.3234$
V	S_1 (Before fiber) $-$ S_1 (After fiber) $= 0.4246$
D	S_2 (Before fiber) $-$ S_2 (After fiber) $= 0.3902$
A	S_2 (Before fiber) $-$ S_2 (After fiber) $= 0.2983$

The polarizations were not retained before and after passing the optical fiber for all of the experimental trials, differing by a range of 0.2983 – 0.4246, indicating the necessity to stabilize the polarization.

Additionally, the 0° QWP angle for the H polarization before and after transmission along the optical fiber are shown by Figure 2. The peaks of the three triggered pulses differ in a range of 2-3 volts in Figure 2A and Figure 2B, demonstrating the change in polarization caused by the optical fiber.

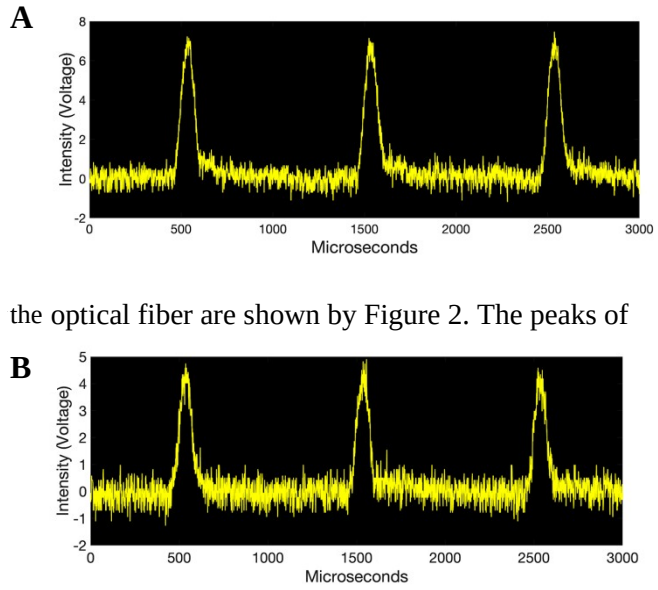

Figure 2: QWP Angle Set to 0° after H applied input. A) Intensity of light before passing fiber. B) Intensity of light after passing fiber. Image developed by student author.

Stabilization of H, V, D, and A

Figure 3 illustrates the setup comprising a QWP and HWP to compensate for the change in polarization. Eq. 11 was used to determine the required angles necessary to stabilize the polarization. S_{in} was assigned to the Stokes parameters after passing the fiber as a 4x1 Stokes matrix entering the QWP and HWP setup. S_{in} was multiplied by Eq. 14 in order to calculate the required QWP and HWP angles necessary to determine S_{out}, which is given by the theoretical Stokes parameters. The required angles, θ_1 and θ_2, along with the stabilized Stokes parameter are shown by Table 2.

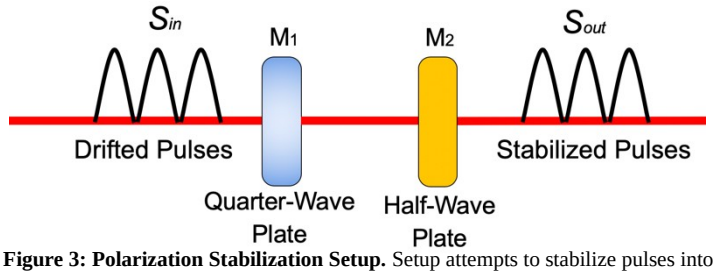

Figure 3: Polarization Stabilization Setup. Setup attempts to stabilize pulses into the theoretical Stokes parameters. Image developed by student author.

Table 2. Polarization Stabilization

Polarization	θ_1	θ_2	Stabilization
H	63.24°	30.52°	$S_1 = 0.9234$
V	122.83°	40.19°	$S_1 = -0.8934$
D	44.61°	87.04°	$S_2 = 0.9095$
A	92.20°	107.31°	$S_2 = -0.8727$

After the drifted pulses were transmitted through the QWP and HWP, the polarization was altered to values closer to the theoretical Stokes parameters, ranging from 0.0766 - 0.1273, indicating that the setup may be used to stabilize light polarization to a more accurate convention. The Poincaré sphere of the drifted and stabilized polarizations are shown in Figure 4. The black arrows indicate the respective Stokes parameter which passed through the QWP and HWP setup, S_{in}. The stabilized polarization is shown by the colored arrows, S_{out}. The length of each of the vectors increased to a point

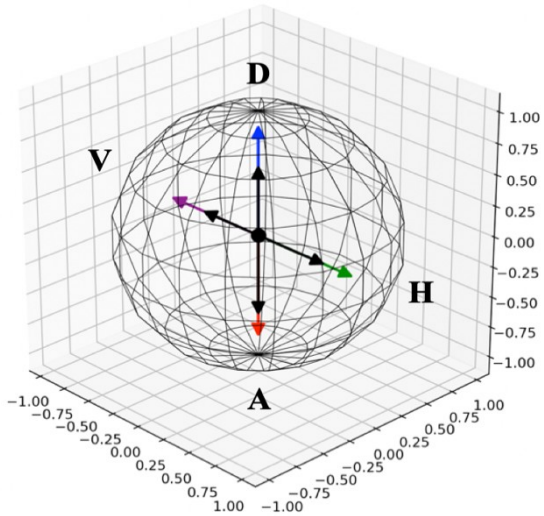

Figure 4: Poincaré Sphere Notation of Altered Polarization. The black arrows indicate S_{in} (drifted polarization) and the colored arrows indicate S_{out} (experimentally stabilized polarization) Image developed by student author.

closer to the surface of the sphere, indicating that the stabilizing setup was able to alter the polarizations more desirable values.

4. CONCLUSIONS:

This study developed a means to characterize and stabilize light polarization states. The characterization setup is easily adjustable, as the standard photodetector may be replaced with a SPCM and vice versa in order to characterize distinct properties of applied polarization inputs [32-34]. Additionally, the polarization is easily outputted using the BFC and FT computational analysis developed in the study and may be compared to one another in order to ensure accuracy and precision of the characterization. The stabilization setup is easily constructed and can compensate for the drift in polarization by calculating θ_1 and θ_2 using Eq. 14.

Future Investigations

The setups may be automatically integrated in order to simultaneously characterize and stabilize the polarization states. To realize this, two components are necessary to construct: a means to rapidly turn wave plates and a method to directly store the associated angle and intensity to output the Stokes parameters. An Arduino may be constructed to automatically program the wave plate to turn a specific step size for a particular duration of time and detect the associated intensity for each angle. This would require using high speed motors connected to the program. Jugetek stepper motors with a driver are possible tools to feasibly perform this operation [35]. This would allow for the same program to connect to the stabilization setup in order to directly calculate the necessary angles of the QWP and HWP and automatically turn the wave plates to its required orientation. Figure 5 shows the potential system. The system would aid in stabilizing arbitrary drifts within the fiber that may occur after characterizing the polarization. Additionally, the efficiency in measuring and stabilizing the polarization would be vastly improved, allowing for direct confirmation and stabilization of applied inputs.

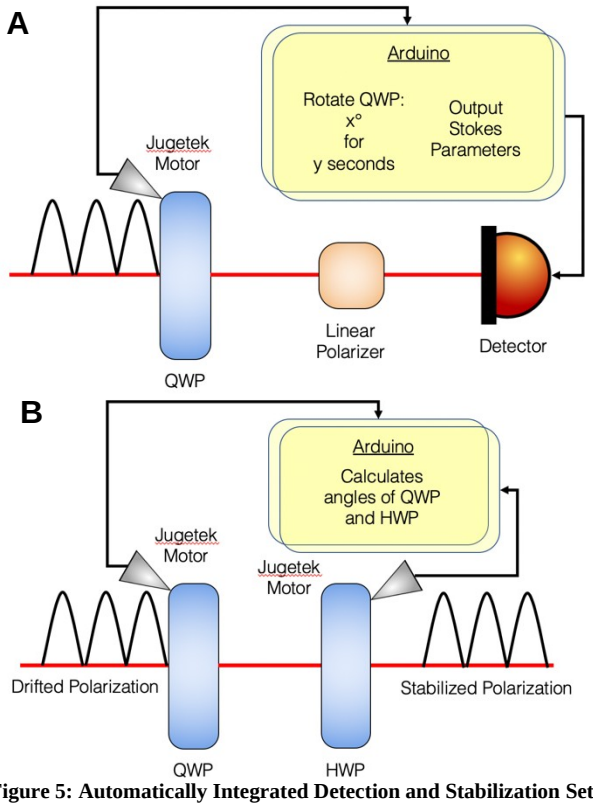

Figure 5: Automatically Integrated Detection and Stabilization Setups. A) Arduino is able to program the Jugetek stepper motor to rotate at a particular speed and interval and measure the Stokes parameters B) Arduino determine the required QWP and HWP angles for stabilizing polarization. Image developed by student author.

Applications

The characterization and stabilization setup can be applied to improve a variety of disciplines. For example, optical activity is the property of polymers to rotate a plane of polarized light. The amount of rotation can be measured by the characterization setup and compared to the theoretical change in polarization after light passes through the polymer to determine the optical activity, which is essential in content determination, purity, and quality standards in products that utilize sugars, amino acids, antibiotics, hydrocarbons, etc [36-38].

Measuring the polarization also has applications in determining biological structures of eye tissues, cellular monolayers, mucous membrane, and skin layers. When exposed to polarized light, the degree of polarization remains detectable even when the structures are considerably thick [37-40]. Information regarding the tissue structures could be determined by measuring the transformation of the

polarization state in scattered images. Additionally, unstained microstructures of cancerous tissue can be analyzed through polarization imaging to determine tissue behaviors [41-43], improving the potential for breakthroughs in cancer research.

Polarized photon pulses are also an essential component of quantum mechanics. The polarization is the information support of a qubit in an optical approach to quantum computing, cryptography, and teleportation. Without a retained polarization state, qubits are susceptible to collapsing, thereby losing the information intended to carry [44-48]. The characterization setup is able to measure the polarization of single photon pulses through the use of the SPCM to confirm polarization qubit orthogonality. This ensures that polarization qubit states are preserved. Additionally, the optical approach to quantum computing has been globally recognized due to its advantageous properties of large-scale generation and connectivity between memory devices in a network of quantum devices through the use of optical fibers [48,49]. Polarized photons are typically sent in single-mode optical fibers to transmit information but are susceptible to drift. The stabilization setup may be used to preserve the orthogonality of the photons that drift within the fiber [50] in order to ensure that the photons can retain and transmit information.

5. APPENDIX:

```
%.....................................................
% finding Stokes by fitting the function for the points
% Fit: 'filename'.
[xData, yData] = prepareCurveData( angle, intensity );

% Set up fittype and options.
ft = fittype( '(1/2)*((SF10+SF11/2)+SF13*sind(2*x)+(SF11/2)*cosd(4*x)+(SF12/2)*sind(4*x))', 'independent', 'x', 'dependent', 'y' );
opts = fitoptions( ft );
opts.Display = 'off';
opts.Lower = [-Inf -Inf -Inf -Inf];
opts.StartPoint = [748.151592823709 0.450541598502498 0.0838213779969326 0.228976968716819];
opts.Upper = [Inf Inf Inf Inf];

% Fit model to data.
[fitresult, gof] = fit( xData, yData, ft, opts );
coef=coeffvalues(fitresult);
SF10=coef(1);
SF11=coef(2);
SF12=coef(3);
SF13=coef(4);
% Plot fit with data.
figure( 'Name', filename );
h = plot( fitresult, xData, yData );
legend( h, 'intensity vs. angle', filename, 'Location', 'NorthEast' );
% Label axes
xlabel( 'angle' );
ylabel( 'intensity' );
grid on
SF0=SF10/SF10;
SF1=SF11/SF10;
SF2=SF12/SF10;
SF3=SF13/SF10;
SF=[SF0 SF1 SF2 SF3];
```

Appendix 1: Best Fit Curve Regression for Angle and Intensity Plot on MATLAB. Fitted regression is plotted as the ft equation. SF10-13 are assigned to the coefficients (coef) to determine the Stokes parameters.

```
stokesdata=H;
%stokesdata=xlsread(filename);
angle=stokesdata(:,1);
    intensity=stokesdata(:,2);
   % plot(angle,intensity,'.')
N=length(angle);
A=(2/N)*sum(intensity);
B=(4/N)*sum(intensity.*sind(2*angle));
C=(4/N)*sum(intensity.*cosd(4*angle));
D=(4/N)*sum(intensity.*sind(4*angle));
S10=A-C;
S11=2*C;
S12=2*D;
S13=B;
S0=S10/S10;
S1=S11/S10;
S2=S12/S10;
S3=S13/S10;

S=[S0 S1 S2 S3];
```

Appendix 2: Fourier transformation calculations on MATLAB. Equations used to determine the polarization. The outputs are compared to BFC.

```
if (abs(P-1)<.05)
    %'The Stokes Matrix is:'
   % S
    %'the light is'
    %S1^2*100, '% linear polarized'
    %S2^2*100, '%  45 linear polarized'
    %S3^2*100, '% circular polarized'
   % 'with a degree of Polarization:'
   % P
   fprintf('************************\n');
   fprintf('****Polarized Light*****\n');
   fprintf('************************\n');
   fprintf('The FT Stokes Matrix is: (%2.4f, %2.4f, %2.4f, %2.4f) \n' ,S);
   fprintf('The FITTED Stokes Matrix is: (%2.4f, %2.4f, %2.4f, %2.4f) \n' ,SF);
   fprintf('%3.4f /// %3.4f %% linear polarized\n' , S1^2*100, SF1^2*100);
   fprintf('%3.4f /// %3.4f %% 45 degree linear polarized\n' , S2^2*100, SF2^2*100);
   fprintf('%3.4f /// %3.4f %% circular polarized\n' , S3^2*100, SF3^2*100);
   fprintf(' with a degree of polrization: %3.4f, %3.4f\n' , P, PF);
   fprintf('\n by getting rid of the unpolarized part, we have:\n');
   fprintf('the FT polarized stokes parameters are:\n(%2.4f, %2.4f, %2.4f, %2.4f)\n',SP)
   fprintf('The FITTED Stokes Matrix is:\n (%2.4f, %2.4f, %2.4f, %2.4f) \n' ,SPF);
   fprintf('%3.3f /// %3.3f %% linear polarized\n' , SP1^2*100, SPF1^2*100);
   fprintf('%3.3f /// %3.3f %% 45 degree linear polarized\n' , SP2^2*100, SPF2^2*100);
   fprintf('%3.3f /// %3.3f %% circular polarized\n' , SP3^2*100, SPF3^2*100);
   fprintf('************************\n');
   fprintf('************************\n');
   % plot(angle,intensity)
else
      fprintf('**********************************\n');
      fprintf('****Partially Polarized Light*****\n');
      fprintf('**********************************\n');
     fprintf('degree of polarization is %3.4f, %3.4f\n', P, PF);
     fprintf('so the light is partially polarized. the FT polarized stokes parameters are:\n(%2.4f, %2.4f, %2.4f, %2.4f)\n',SP)
     fprintf('The FITTED Stokes Matrix is:\n (%2.4f, %2.4f, %2.4f, %2.4f) \n' ,SPF);
```

<u>Appendix 3</u>: Percent Polarization Outputs.

References

[1] E. Hecht, Optics. San Francisco: Addison Wesley, 2002, pp. 325-379
[2] C. F. Bohren, D. R. Huffman, Absortion and Scattering of Light by Small Particles, New York:Wiley, 1983.
[3] W. Osten, ed. Optical Inspection of Microsystems (CRC Press, 2006).
[4] J. W. Maseberg and T. J. Gay, Journal of Physics B: Atomic, Molecular and Optical Physics 39, 4861 (2006).
[5] M. Losurdo, M. Bergmair, G. Bruno, D. Catellan, C. Cobet, A. de Martino, K. Fleischer, Z. Dohcevic-Mitrovic, N. Esser, M. Gaillet, R. Gajic, D. Hemzal, K. Hingerl, J. Humlíček, R. Ossikovski, Z. V. Popovic, and O. Saxl, "Spectroscopic ellipsometry and polarimetry for materials and systems analysis at the nanometer scale: state of the art, potential, and perspectives," J. Nanopart. Res. 11, 1521–1554 (2009).
[6] J. S. Baba, J.-R. Chung, A. H. DeLaughter, B. D. Cameron, and G. L. Cote, "Development and calibration of an automated Mueller matrix polarization imaging system," J. Biomed. Opt. 7, 341–349 (2002).
[7] R. W. Collins and J. Koh, "Dual rotating-compensator multichannel.
[8] Saadon, H., Théofanous, N., Aillerie, M. and Fontana, M. (2006). Thermo-optic effects in electro-optic crystals used in an intensity-modulation system. – Application in LiTaO3. *Applied Physics B*, 83(4), pp.609-617.
[9] Turchette, Q.A., Hood, C.J., Lange, W., Mabuchi, H., and Kimble, H.J., "Measurement of Conditional Phase Shifts for Quantum Logic", Phys. Rev. Lett. 75, 4710-4713 (1995).
[10] Franson, J.D., "Cooperative Enhancement of Optical Quantum Gates", Phys. Rev. Lett. 78, 3852-3855 (1997).
[11] Knill, E., LaFlamme, R., and Milburn, G.J., "A scheme for efficient quantum computation with linear optics", Nature 409, 46-52 (2001).
[12] Pittman, T.B., Jacobs, B.C., and Franson, J.D., "Demonstration of feed-forward control for linear optics quantum computation", Phys. Rev. A 66, 052305 (2002).
[13] Franson, J.D., Donegan, M.M., Fitch, M.J., Jacobs, B.C., and Pittman, T.B., "High Fidelity Quantum Logic Operations using Linear Optical Elements", Phys. Rev. Lett. 89, 137901 (2004).
[14] Pittman, T.B., Jacobs, B.C., and Franson, J.D., "Probabilistic quantum logic operations using polarizing beam splitters", Phys. Rev. A 64, 062311 (2001). 13
[15] Einstein, A., Podolsky, B., and Rosen, N., "Can Quantum Mechanical Description of Physical Reality be Considered Complete?", Phys. Rev. 48, 696-702 (1935).
[16] Pittman, T.B. and Franson, J.D., "Violation of Bell's Inequality with Photons from Independent Sources", Phys. Rev. Lett. 90, 24041 (2003).
[17] Pittman, T.B., Fitch, M.J., Jacobs, B.C., and Franson, J.D., "Experimental Controlled-NOT logic gate for single photons in the coincidence basis", Phys. Rev. A 68, 032316 (2003).
[18]. D.N. Klyshko, Photons and Nonlinear Optics, Gordon and Breach Science, New York (1988).
[19] Pittman, T.B., Jacobs, B.C., and Franson, J.D., "Demonstration of non-deterministic quantum logic operations using linear optical elements", Phys. Rev. Lett. 88, 257902 (2002).
[20] Pittman, T.B., Jacobs, B.C., and Franson, J.D., "Probabilistic quantum encoder for single-photon qubits", Phys. Rev. A 69, 042306 (2004).
[21] C. Williams, Explorations in quantum computing. London: Springer, 2011.
[22] "Quantum technology – popular science description", 2018. [Online]. Available: https://www.chalmers.se/en/news/Documents/quantum_technology_popdescr_171114_eng.pdf.
[23] H. Pichler, S. Choi, P. Zoller and M. Lukin, "Universal photonic quantum computation via time-delayed feedback", 2018. .

[24] J. Tyo, D. Goldstein, D. Chenault and J. Shaw, "Review of passive imaging polarimetry for remote sensing applications", *Applied Optics*, vol. 45, no. 22, p. 5453, 2006.
[25] R. Azzam, "Stokes-vector and Mueller-matrix polarimetry [Invited]", *Journal of the Optical Society of America A*, vol. 33, no. 7, p. 1396, 2016.
[26] J. Tyo, "Noise equalization in Stokes parameter images obtained by use of variable-retardance polarimeters", *Optics Letters*, vol. 25, no. 16, p. 1198, 2000.
[27] A. Peinado, A. Lizana, J. Vidal, C. Iemmi and J. Campos, "Optimization and performance criteria of a Stokes polarimeter based on two variable retarders", *Optics Express*, vol. 18, no. 10, p. 9815, 2010.
[28] S. Roy, O. Awartani, P. Sen, B. O'Connor and M. Kudenov, "Intrinsic coincident linear polarimetry using stacked organic photovoltaics", *Optics Express*, vol. 24, no. 13, p. 14737, 2016.
[29] G. Topasna and D. M., "Stokes parameters in undergraduate laboratory exercises", *Education and Training in Optics and Photonics*, 2009.
[30] Z. Kopal, *Advances in astronomy and astrophysics.*. New York, N.Y.: Academic Press, 1965.
[31] S. Li, N. Quan, C. Zhang, T. Mu and B. Hu, "Stokes polarimeter for the measurement of full linearly Stokes parameters with immunity to Gaussian and Poisson noise", *Optik*, vol. 175, pp. 8-16, 2018.
[32] A. Ling, K. Soh, A. Lamas-Linares and C. Kurtsiefer, "An optimal photon counting polarimeter", *Journal of Modern Optics*, vol. 53, no. 10, pp. 1523-1528, 2006.
[33] S. Kawabata, "High-speed Transmission type Four Detectors Polarimeter and its Applications", 2018. .
[34] J. Mueller, K. Leosson and F. Capasso, "An Ultra-compact In-line Polarimeter", *Optica*, 2015.
[35] "The Applications of Polarimeters", 2018. [Online]. Available: https://www.glascol.com/applications-of-polarimeters.
[36] *Www-inst.eecs.berkeley.edu*, 2018. [Online]. Available: http://www-inst.eecs.berkeley.edu/~cs191/sp12/notes/chap1&2.pdf.
[37] G. Topasna and D. M., "Stokes parameters in undergraduate laboratory exercises", *Education and Training in Optics and Photonics*, 2009.
[38] "The Applications of Polarimeters", 2018. [Online]. Available: https://www.glascol.com/applications-of-polarimeters.
[39] K. Kraus, States, Effects and Operations. Fundamental Notions of Quantum Theory, Lecture Notes in Physics Vol. 190 (Springer-Verlag, Berlin, 1983).
[40] B.-G. Englert, K. M. Tin, C. G. Goh, and H. K. Ng, Laser Phys. 15, 7 (2005).
[41] J.R. Ashburn, R.A. Cline, P.J.M. Vanderburgt, W.B. Westerveld and J.S. Risley, "Experimentally determined density-matrices for H(n=3) formed in H+-He collisions from 20 to 100 keV," Phys. Rev. A 41, 2407-2421 (1990).
[42] D. T. Smithey, M. Beck, M. G. Raymer and A. Faridani, "Measurement of the Wigner distribution and the density matrix of a light mode using optical homodyne tomography: Application to squeezed states and the vacuum," Phys. Rev. Lett. 70, 1244 (1993).
[43] G. Breitenbach, S. Schiller, J. Mlynek, "Measurement of the quantum states of squeezed light," Nature 387, 471-475 (1997).
[44] M. A. Nielsen and I. L. Chuang, Quantum Computation and Quantum Information (Cambridge University Press, Cambridge, 2000), ch.11.
[45] A. Uhlmann, Rep. Math. Phys. 9, 273 (1976).
[46] S. Gaertner, H. Weinfurter, and C. Kurtsiefer, Rev. Sci. Inst. 76, 123108 (2005).
[47] S. Massar and S. Popescu, Phys. Rev. Lett. 74 (8), 1259 (1995).
[48] R. Derka, V. Bu˘zek, and A. K. Ekert, Phys. Rev. Lett. 80 (8), 1571 (1998).
[49] J. I. Latorre, P. Pascual, and R. Tarrach, Phys. Rev. Lett. 81 (7), 1351 (1998).
[50] R. D. Gill and S. Massar, Phys. Rev. A 61, 042312 (2000).